Artigo

APPLICATIONS OF NMR AND THEORETICAL CALCULATIONS TO STUDY THE O-H···N INTRAMOLECULAR HYDROGEN BOND EFFECT ON THE CONFORMATIONAL EQUILIBRIUM OF *CIS*-3-*N*-ETHYLAMINOCYCLOHEXANOL AND *CIS*-3-*N,N*-DIETHYLAMINOCYCLOHEXANOL

Paulo R. de Oliveira[a,*], Roberto Rittner[b], Palimecio G. Guerrero Jr.[a], Patrick R. Batista[b] and Gustavo J. Costa[c]
[a]Departamento Acadêmico de Química e Biologia, Universidade Tecnológica Federal do Paraná, 81280-340 Curitiba – PR, Brasil
[b]Instituto de Química, Universidade Estadual de Campinas, 13083-970 Campinas – SP, Brasil
[c]Departamento de Química Fundamental, Instituto de Química, Universidade de São Paulo, 05508-000 São Paulo – SP, Brasil

Recebido em 31/05/2022; aceito em 21/03/2023; publicado na web 12/05/2023

Textbooks show that in *cis*-1,3-disubstituted cyclohexane molecule, the conformer with the substituents in the diaxial positions is higher in energy and hence, it presents a low population in the conformational equilibrium. The diaxial conformer is destabilized by the repulsion between the substituent groups and the axial hydrogen atoms on the same side of the ring. This interaction is known as the 1,3-diaxial interaction. In this study, the solvent effect on the conformational equilibria of *cis*-3-*N*-ethylaminocyclohexanol (*cis*-3-EACOL) and *cis*-3-*N,N*-diethylaminocyclohexanol (*cis*-3-DEACOL) has been assessed through the spin-spin coupling constant ($^3J_{HH}$). The results show that the diaxial conformation of *cis*-3-EACOL decreases from 92% in CCl_4 ($\Delta G_{ee\text{-}aa}$ = 1.48 kcal mol^{-1}) to 10% in DMSO-d_6 ($\Delta G_{ee\text{-}aa}$ = −1.31 kcal mol^{-1}). For *cis*-3-DEACOL the diaxial conformer decreased from 36% in CCl_4 ($\Delta G_{ee\text{-}aa}$ = −0.33 kcal mol^{-1}) to 7% in Pyridine-d_5 ($\Delta G_{ee\text{-}aa}$ = −1.55 kcal mol^{-1}). The stabilization of the diaxial conformer in nonpolar solvents takes place due to the O-H···N intramolecular hydrogen bond, which overcomes the 1,3-diaxial steric interactions.

Keywords: conformational analysis; intramolecular hydrogen bond; aminocyclohexanols; QTAIM; NCI.

INTRODUCTION

The conformational analysis performed by Sachse resulted in the discovery of two conformations of cyclohexane, known as chair and boat.[1] Based on his findings, many studies have been conducted to describe the conformational preferences, electronic, steric, and dipole-dipole effects that influence the conformational equilibrium of a molecule.[2-6] Besides that, the hydrogen bond (HB) is also known to play a key role in determining the three-dimensional structure adopted by proteins, nucleic acids, and amino acids.[7-9] So, many conformational studies of amino compounds[10-13] such as amino acids have been reported.[12-16] HBs are also recognized as contributors to the spectroscopic features such as proton chemical shifts.[17] Also, the HB energy can be fine-tuned by changes in the aromatic character of a molecule. HBs that increase aromaticity are strengthened, and those that reduce aromaticity are weakened.[18-19] The role of the intramolecular HB (IAHB) also have been investigated,[10,12,20,21] and recently was reported as very important for the stability of most conformers of vitamin C,[22] as well as in the isotopic effect studies.[23]

In previous work,[24] it was demonstrated that *syn*-1,3-diaxial steric effects favor diequatorial conformation in the equilibria of *cis*-3-X-cyclohexanols (X = Cl, Br, I, CH_3) and 3-X-1-methoxycyclohexanes (X = F, Cl, Br, I, CH_3). However, the presence of some substituents on the six-membered ring has shown that it is possible to promote the diaxial conformer through the IAHB. Studies of *cis*-3-methoxy-[25] and *cis*-3-ethoxy-cyclohexanols,[26] revealed that IAHBs are responsible for stabilizing the diaxial conformation, overcoming 1,3-diaxial steric interactions. Oliveira and Rittner[27] also have shown that the larger the size and the indutive effect of alkoxy groups, the greater the intensity of IAHB interaction through investigations of *cis*-3-alkoxycyclohexanols molecules.

Therefore, aiming to extend the investigations from those results obtained in previous work,[28] we concentrate our efforts to probe the solvent effect on the conformational equilibrium of *cis*-3-*N*-ethylaminocyclohexanol (*cis*-3-EACOL) and *cis*-3-*N,N*-diethylaminocyclohexanol (*cis*-3-DEACOL) (Figure 1), using ^{1}H NMR and theoretical calculations based on density functional theory (DFT) framework. The O-H···N IAHB is also investigated by theoretical calculations in the gas phase to probe the extent of its stability concerning to the size of the amino group substituent.

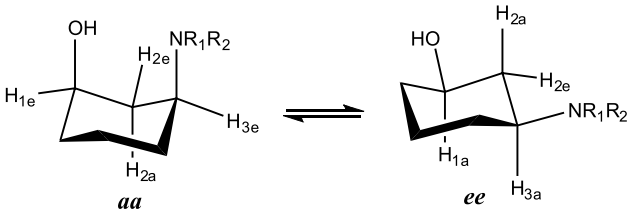

R_1=CH_2CH_3, R_2=H or R_1=R_2=CH_2CH_3

Figure 1. *Conformational equilibrium between diaxial (aa) and diequatorial (ee) conformations for cis-3-EACOL (R_1=CH_2CH_3, R_2=H) and cis-3-DEACOL (R_1=R_2=CH_2CH_3)*

EXPERIMENTAL

Synthesis

Anhydrous ethylamine: 100 mL of 70% ethylamine solution was slowly dropped (ca. 2 h) onto 70 g of sodium hydroxide contained in a 250 mL three-neck round-bottomed flask, equipped with a Vigreux micro-distilling apparatus including a collecting flask cooled to −30 °C to prevent loss of the ethylamine (b.p. 17 °C).

Cis-3-EACOL (1): 35 mL of anhydrous ethylamine was placed in a round-bottomed flask fitted with a magnetic stirrer at −25 ºC, 2.0 g of 2-cyclohexen-1-one was added dropwise, and the reaction

*e-mail: poliveira@utfpr.edu.br

mixture was stirred at −25 ºC for 2 h. The excess of ethylamine was evaporated at room temperature. The product obtained (3-*N*-ethylaminocyclohexanone) was added dropwise to a three-necked 250-mL round-bottomed flask containing a suspension of lithium aluminum hydride (0.4 g, 0.11 mmol) in tetrahydrofuran (60 mL), with stirring, at −10 ºC and in a nitrogen atmosphere. The mixture was allowed to warm to room temperature and was stirred for one more hour. Water was added dropwise to destroy the excess lithium aluminum hydride. The organic layer was separated with diethyl ether, dried over $MgSO_4$, filtered, and the solvent evaporated. The compound was purified by column chromatography, using hexane:ethyl acetate 10:1 as eluent and 230-400 mesh silica gel to eliminate the 2-cyclohexen-1-ol. Next, methanol was used to obtain 2.1 g (72%) of *cis*-3-EACOL.

Cis-3-DEACOL (2): 35 mL of diethylamine 98% was placed in a round-bottomed flask fitted with a magnetic stirrer at 25 ºC, 20 g of 2-cyclohexen-1-one was added dropwise, and the reaction mixture was stirred at 25 ºC for 15 h. Excess diethylamine was evaporated in a rotary evaporator. The product obtained (3-*N*,*N*-diethylaminocyclohexanone) was reduced by the same method used for *cis*-3-EACOL, replacing 3-*N*-ethylaminocyclohexanone by 3-*N*,*N*-diethylaminocyclohexanone, resulting in 18.5 g (52%) of *cis*-3-DEACOL.

NMR spectroscopy

The ^{1}H NMR spectra were recorded on an INOVA 500 spectrometer with probe temperature of 20 °C, operated at 499.88 (^{1}H) and 125.70 MHz (^{13}C) or on a Varian Gemini 300 spectrometer operating at 300.07 (^{1}H) and 75.45 MHz (^{13}C). In all cases, $SiMe_4$ (TMS) was used as an internal reference. To characterize the compounds synthetized the assignment of the signals in ^{1}H and ^{13}C NMR spectra of the *cis* isomers of the two compounds, were recorded at concentrations of 0.30 mol L^{-1} using $CDCl_3$ as solvent.

Cis-3-EACOL: ^{1}H NMR (300 MHz, $CDCl_3$), δ 3.80 (tt, 6.86, 3.43, 1H), 2.81 (tt, 6.69, 3.36, 1H), 2.68 (m, 2H), 1.90 (m, 1H), 1.80 (m, 1H), 1.69 (m, 1H), 1.57 (m, 1H), 1.37 (m, 2H), 1.32 (m, 2H), 1.12 (t, 7.16, 3H). ^{13}C NMR (125 MHz, $CDCl_3$), δ 68.6, 54.4, 50.1, 41.3, 34.2, 31.8, 19.2, 15.2.

Cis-3-DEACOL: ^{1}H NMR (500 MHz, $CDCl_3$), δ 3.68 (tt, 9.01, 4.15, 1H), 2.63 (m, 1H), 2.58 (m, 4H), 1.92 (m, 1H), 1.82 (m, 2H), 1.66 (m, 1H), 1.49 (m, 1H), 1.36 (m, 1H), 1.30 (m, 1H), 1.27 (m, 1H), 1.02 (t, 7.16, 6H). ^{13}C NMR (125 MHz, $CDCl_3$), δ 69.7, 56.7, 43.0, 36.8, 35.1, 28.1, 20.8, 12.7.

The assessment of the solvent effect on conformational equilibria of the compounds was carried out recording the spectra at concentrations of 0.05 mol L^{-1} in CCl_4, $CDCl_3$, $C_2D_2Cl_4$, CD_3CN, acetone-d_6, pyridine-d_5, and DMSO-d_6.

Computational details

The conformational search in gas phase was carried out using molecular mechanics with MM3 method using the TINKER software.[29] All conformer geometries were optimized in gas phase and solvent regime along the frequency calculations using the DFT M06-2X,[30] functional, which is recommended for an accurate description of non-covalent interactions and performed quite well for a system with dispersion and ionic HB interactions,[31] such as for amino compounds.[10] As the basis set, the triple-ζ 6-311++G(3df,3pd)[32] was chosen to yield a reliable description of the orbitals. It includes diffuse functions on all atoms and supplemented by d,f-polarizations functions on heavy atoms (C, N, and O), and p,d-polarization functions on hydrogens atoms. Spin-spin coupling constant ($^3J_{HH}$) were calculated in the gas phase using the B3LYP,[33-36] functional and the EPR-III,[37] basis set. This basis set includes *s*-functions with high exponentials by parametrization for a better description of the nuclear region, being a good choice for NMR parameters. In addition, it is optimized for the computation of hyperfine coupling constants by DFT methods, particularly B3LYP.[38,39] The solvent effect was represented by the continuum polarizable model SMD[40] in the optimization and NMR calculations. Note that in the SMD formalism, the solute is embedded in a cavity surrounded by a polarizable medium with the dielectric constant of specific solvent, forming the solvent reaction field. In this case, superpositions of nuclear-centered spheres form the solvent cavity and the full solute electron density is used instead of partial atomic charges definition. The calculations were performed using the Gaussian09 program package, revision D.01.[41]

Natural bond orbital analysis (NBO 6.0)[42] was performed at the M06-2X/6-311++G(3df,3pd) level of theory for hyperconjugative and steric interactions (using the keyword "steric"). Topological analysis was carried out with the Quantum Theory Atoms in Molecules (QTAIM)[43] and Non-Covalent Interaction (NCI) methods, using the AIMALL,[44] and NCIPLOT 3.0[45] programs, respectively.

RESULTS AND DISCUSSION

Conformational analysis

The conformational search of *cis*-3-EACOL and *cis*-3-DEACOL provided 27 and 34 rotamers, respectively. For *cis*-3-EACOL, 4 rotamers were diaxial (aa) and 23 diequatorial (ee), whereas for *cis*-3-DEACOL, 7 rotamers were aa and 27 ee. The thermal populations and Gibbs relative energies of the conformers with $\Delta G < 2.0$ kcal mol^{-1} are presented in Table 1. Those with $\Delta G > 2.0$ kcal mol^{-1} were not considered, since they comprise a very small proportion in the equilibrium.

In Figure 2 the most stable rotamers for *cis*-3-EACOL (1aa3 and 1ee18) and for *cis*-3-DEACOL (2aa7 and 2ee17) are depicted. The 1aa3 and 2aa7 rotamers showed the IAHB O_7-H_8···N_9. The substituent groups of the 1ee18 and 2ee17 rotamers were seen to be as far as possible from the ring, reducing the steric effect. Using the Gibbs energy values for the conformational equilibrium, the molar fractions of the aa and ee conformers were calculated (Table 2).

The population of aa conformation for *cis*-3-EACOL and *cis*-3-DEACOL compounds in the gas phase were 96% ($\Delta G = 1.80$ kcal mol^{-1}) and 41% ($\Delta G = -0.22$ kcal mol^{-1}), respectively. These results indicate that in the *cis*-3-EACOL, the equilibrium is shifted to the conformer aa, whereas the change to a tertiary amino group increases the 1,3-diaxial steric effect and, in turn, the conformer with diethyl groups in equatorial position predominates. It is noteworthy that the entropy term ($T\Delta S$) in Table 2 is the parameter responsible for conformational preference in the equilibria, since the enthalpy terms are very similar for both compounds. Thus, as the $T\Delta S > 0$, the repulsive interactions in aa conformer is quite significant and, therefore, there is more entropy in the ee conformer (energetically favorable to access more rotamers - freedom of movement). Although, the aa conformer seems to be more stabilized by IAHB, which decreases the entropy term for *cis*-3-EACOL. On the other hand, the IAHB formation must be sterically more hindered in the *cis*-3-DEACOL, increasing the ee conformer stability and, hence, the entropy. Several works have also addressed the role of thermodynamic terms in substituted cyclohexanes, which were brought together in a review.[46]

Koch and Popelier,[47] showed that the existence of the hydrogen bond can be confirmed if it satisfies eight criteria. The topological

Table 1. Relative Gibbs free energies (ΔG)[a] and thermal population[b] for aa and ee rotamers of *cis*-3-EACOL (1) and *cis*-3-DEACOL (2) calculated at M06-2X/6-311++G(3df,3pd) level of theory in gas phase

Rotamer	ΔG	Thermal Population	Rotamer	ΔG	Thermal Population	Rotamer	ΔG	Thermal Population	Rotamer	ΔG	Thermal Population
1aa1	1.93	3.8	1ee11	1.81	1.5	2aa1	1.24	8.5	2ee11	0.93	6.6
1aa2	0.86	22.2	1ee12	1.81	1.2	2aa2	1.23	8.5	2ee12	1.08	4.0
1aa3	0.00	69.8	1ee13	0.54	4.1	2aa3	1.76	4.0	2ee13	1.85	1.8
1aa4	1.95	4.2	1ee14	1.56	1.6	2aa4	1.39	5.2	2ee14	1.89	1.0
1ee1	1.63	1.7	1ee15	0.27	5.7	2aa5	1.40	5.2	2ee15	1.79	1.7
1ee2	0.24	8.7	1ee16	1.86	1.2	2aa6	1.27	12.9	2ee16	1.52	2.3
1ee3	1.55	1.6	1ee17	0.57	4.4	2aa7	0.00	55.6	2ee17	0.00	22.5
1ee4	0.23	7.8	1ee18	0.00	12.2	2ee1	0.18	16.2	2ee18	1.89	1.5
1ee5	1.79	1.3	1ee19	1.76	1.5	2ee2	1.90	1.0	2ee19	1.25	3.5
1ee6	0.32	7.4	1ee20	0.08	11.2	2ee3	1.20	3.9	2ee20	1.24	3.5
1ee7	0.63	3.7	1ee21	1.62	1.5	2ee4	1.21	3.9	2ee21	1.71	1.9
1ee8	0.57	4.2	1ee22	0.18	9.3	2ee5	1.19	3.9	2ee22	1.78	1.5
1ee9	1.92	1.1	1ee23	1.87	1.1	2ee6	1.79	1.9	2ee23	1.87	1.4
1ee10	0.39	6.0	-	-	-	2ee7	1.88	0.9	2ee24	1.93	0.7
-	-	-	-	-	-	2ee8	1.77	1.8	2ee25	1.90	1.2
-	-	-	-	-	-	2ee9	1.89	1.5	2ee26	1.02	3.2
-	-	-	-	-	-	2ee10	1.88	1.5	2ee27	1.00	5.4

[a]In kcal mol^{-1}. [b]In percentage (see supplementary material).

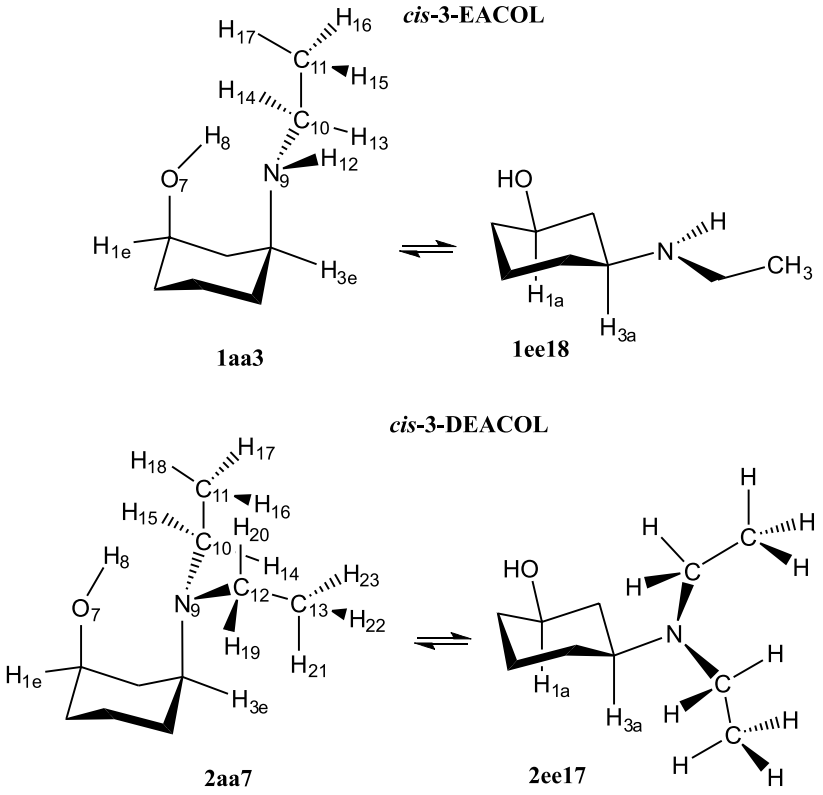

Figure 2. *Most stable rotamers in gas phase for cis-3-EACOL (1aa3 and 1ee18) and cis-3-DEACOL (2aa7 and 2ee17)*

analysis values of the 1aa3 and 2aa7 rotamers using QTAIM analysis (Figure 3) indicated that the IAHB O_7-H_8···N_9 was identified and characterized by the presence of bond path, bond critical point (BCP), and ring critical point (RCP) in both aa conformers (Figures 3a and 3a') and fulfilled all the criteria established by Koch and Popelier (see supplementary material).

NCI analysis also confirmed the presence of the IAHB O_7-H_8···N_9 for the 1aa3 and 2aa7 rotamers. The results are shown in gradient isosurfaces (Figure 3b and 3b') and reduced density gradients (RDG) *versus* sign(λ_2)ρ(r) (Figure 3c and 3c'). Analysis of Figures 3c and 3c' indicated the presence of IAHB O_7-H_8···N_9 in the 1aa3 and 2aa7 rotamers represented by the strong attractive interactions (peaks at

Table 2. Thermodynamic properties[a,b] and aa and ee molar fractions (X_{aa} and X_{ee})[c] for conformational equilibrium of *cis*-3-EACOL (1) and *cis*-3-DEACOL (2) compounds calculated at M06-2X/6-311++G(3df,3pd) level of theory in gas phase

Compound	ΔH	TΔS	ΔG	X_{aa}	X_{ee}
cis-3-EACOL	2.58	0.67	1.91	96	4
cis-3-DEACOL	2.48	2.70	–0.22	41	59

[a]In kcal mol^{-1}. [b]298.15 K, 1 atm. [c]In percentage.

–0.0292 and –0.0310 a.u., respectively). This also are in agreement with our earlier observations obtained by the QTAIM analysis. Negative peaks in Figures 3c and 3c' showed other weak attractive interactions in the 1aa3 and 2aa7 rotamers. The blue color gradients on the isosurfaces (Figures 3b and 3b') confirm the presence of highly attractive interactions between the hydrogen of the hydroxyl group (H_8) and the nitrogen atom (N_9). Positive peaks in Figures 3c and 3c' are related to the repulsive interactions between atoms (green isosurfaces) or between antibonding orbitals (red isosurfaces) for the 1aa3 and 2aa7 rotamers, respectively.

NBO results for the most stable aa rotamers of *cis*-3-EACOL (1aa3) and *cis*-3-DEACOL (2aa7) are shown in Table 3. The orbital interactions are related to the stability of the IAHB O_7-H_8···N_9. The interactions $\sigma C_4 - H_{4a} \rightarrow \sigma^* C_3 - N_9$ and $\sigma C_2 - H_{2a} \rightarrow \sigma^* C_3 - N_9$ are stronger than the interactions $\sigma C_3 - N_9 \rightarrow \sigma^* C_4 - H_{4a}$ and $\sigma C_3 - N_9 \rightarrow \sigma^* C_2 - H_{2a}$ showing the electron donation to the nitrogen. The interactions $\sigma C_{11} - H_{16} \rightarrow \sigma^* N_9 - C_{10}$ and $\sigma C_{13} - H_{22} \rightarrow \sigma^* N_9 - C_{12}$ showed an increase in electron density on the nitrogen to *cis*-3-EACOL and *cis*-3-DEACOL, respectively.

The energy values of the interaction $LP(1)N_9 \rightarrow \sigma^* O_7 - H_8$ showed a higher inductive effect of nitrogen (N_9) in the *cis*-3-DEACOL than *cis*-3-EACOL. The natural localized molecular orbital (NLMO) values summarized in Table 6 showed that the exchange interaction (steric energies)[48] between the bonding orbitals is greater for *cis*-3-DEACOL than for *cis*-3-EACOL because the sum of steric energy in *cis*-3-DEACOL (43.32 kcal mol^{-1}) is higher than in *cis*-3-EACOL (40.94 kcal mol^{-1}).

The strength of the IAHB for *cis*-3-EACOL and *cis*-3-DEACOL compounds was analyzed through the values shown in Table 4. The electronic energy density H(r) in BCP is defined by Equation (1),[49] in which G(r) is the electronic kinetic energy density, which is always positive, and V(r) is the electronic potential energy density and must be negative.

$$H(r)_{BCP} = G(r) + V(r) \quad (1)$$

The dissociation energy of IAHB was obtained by Equation (2):[50]

$$E_{IAHB} = -\frac{1}{2}V(r) \quad (2)$$

Cis-3-DEACOL had the lowest distances between H_8···N_9 and O_7···N_9, the greatest length of the O_7-H_8 bond and angle between the O_7-H_8···N_9 atoms, the most significant displacement stretching frequency of the O_7-H_8 bond (bathochromic shift), as well as most remarkable greatest energy dissociation of the IAHB O-H···N. These results indicate that the strength of IAHB increases from *cis*-3-EACOL to *cis*-3-DEACOL compound. The positive values for $\nabla^2\rho(r)_{BCP}$ and the negative values for H(r) (Table 4) indicate that the IAHB O_7-H_8···N_9 shows electrostatic and covalent characteristics for these compounds.[51]

Solvent effect on the $^3J_{HH}$

The solvent effect was evaluating in order to obtain the preference of each conformer in equilibrium for the *cis* isomer. However, the solvent effect is known to be very reduced for $^3J_{HH}$,[52] and of small geometrical changes source. The $^3J_{H1aH2a}$ and $^3J_{H1eH2e}$ calculated for lowest in energy conformers ee and aa, found after optimization employing the SMD model to describe the solvent effect, for the most non-polar (CCl_4) and polar (DMSO) solvents are shown in Table 5.

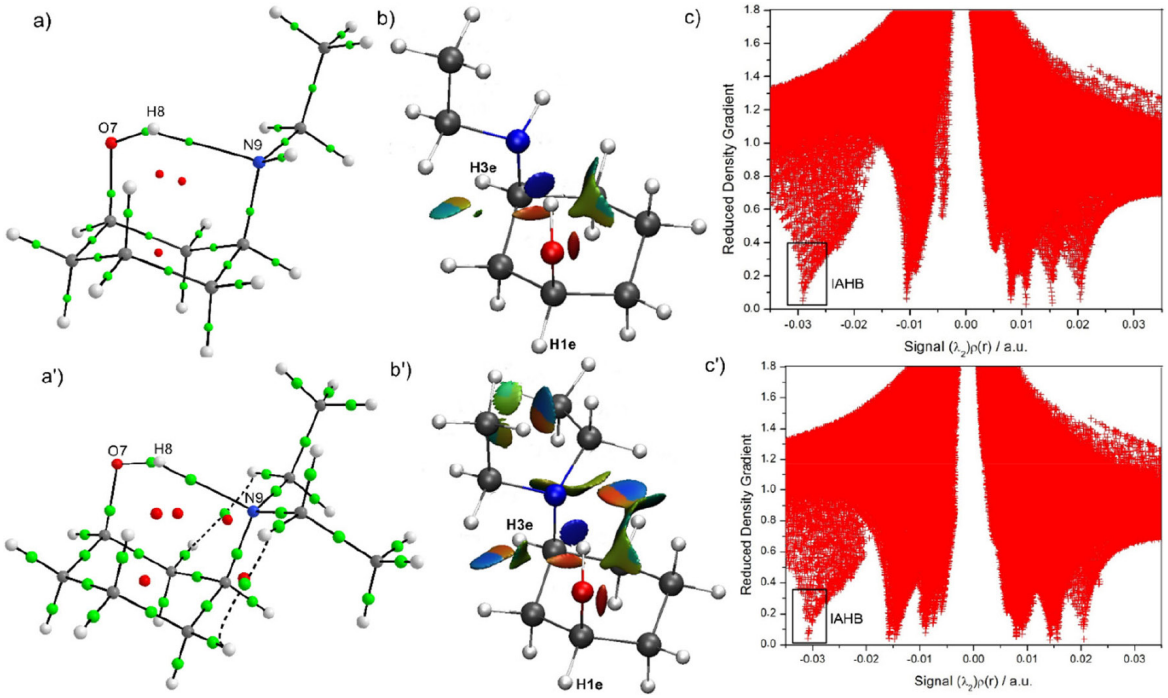

Figure 3. *Topological analysis by QTAIM molecular graphics, NCI isosurfaces = 0.4, and blue-red-green color scale −0.2 < signal (λ_2)ρ(r) < 0.2 a.u. and reduced density gradient graph versus the signal (λ_2)ρ(r) for 1aa3 (a, b and c) and for 2aa7 (a', b', and c') rotamers, respectively*

Table 3. Energies[a,b] of the main NBO electronic and NLMO steric interactions for the most stable aa rotamers of *cis*-3-EACOL (1) and *cis*-3-DEACOL (2) compounds calculated at M06-2X/6-311++G(3df,3pd) level of theory

NBO		Rotamer		NLMO		Rotamer	
Donor	Acceptor	1aa3	2aa7	*i*	*j*	1aa3	2aa7
$LP(1)N_9$	$\sigma^*O_7 - H_8$	8.86	9.09	C_3-C_2	N_9-C_{12}	-	3.26
$\sigma C_4 - H_{4a}$	$\sigma^*C_3 - N_9$	4.58	5.40	C_3-C_4	N_9-C_{12}	-	4.37
$\sigma C_3 - N_9$	$\sigma^*C_4 - H_{4a}$	1.28	1.08	C_3-C_2	N_9-C_{10}	1.47	2.82
$\sigma C_2 - H_{2a}$	$\sigma^*C_3 - N_9$	4.89	5.08	C_3-C_4	N_9-C_{10}	2.94	3.68
$\sigma C_3 - N_9$	$\sigma^*C_2 - H_{2a}$	1.24	1.14	C_3-C_2	N_9-H_{12}	4.37	-
$\sigma C_3 - C_4$	$\sigma^*N_9 - C_{10}$	2.92	2.81	C_3-C_4	N_9-H_{12}	4.49	-
$\sigma N_9 - C_{10}$	$\sigma^*C_3 - C_4$	1.87	2.36	C_3-N_9	C_2-H_{2a}	4.51	5.53
$\sigma C_{10} - C_{11}$	$\sigma^*C_3 - N_9$	3.04	2.88	C_3-N_9	C_4-H_{4a}	4.67	5.67
$\sigma C_3 - N_9$	$\sigma^*C_{10} - C_{11}$	1.14	2.11	C_2-H_{2a}	C_1-O_7	3.74	4.05
$\sigma C_{11} - H_{16}$	$\sigma^*N_9 - C_{10}$	3.88	4.59	C_1-O_7	C_6-H_{6a}	3.91	3.86
$\sigma N_9 - C_{10}$	$\sigma^*C_{11} - H_{16}$	1.14	0.81	C_1-H_{1e}	O_7-H_8	5.35	5.66
-	-	-	-	C_4-H_{4e}	N_9-H_{12}	1.42	-
-	-	-	-	C_2-C_1	O_7-H_8	4.07	4.42
-	-	-	-		TOTAL[c]	40.94	43.32

[a]In kcal mol^{-1}. [b]298.15 K, 1 atm. [c]Sum of the steric energies in kcal mol^{-1}.

Table 4. Energy potential in BCP V(r), dissociation energy (E_{IAHB}) of O_7–H_8···N_9, the total electronic density in the PCL H(r), kinetic energy density G(r), Laplacian of the electronic density at the BCP, and geometric parameters for the more stable aa rotamers of *cis*-3-EACOL (1) and *cis*-3-DEACOL (2) compounds

Parameter	Rotamer	
	1aa3	2aa7
V(r) (a.u.)	–0.02327	–0.02497
E_{IAHB} (a.u.)	0.01164	0.01248
$H(r)_{BCP}$	$-3.5.10^{-4}$	$-11.8.10^{-4}$
G(r) (a.u.)	0.02292	0.02379
$\nabla^2\rho(r)_{BCP}$ (a.u.)	0.09027	0.09046
Length H_8···N_9 (Å)	1.9870	1.9800
[a]Stretching O_7-H_8 (Å)	0.0083	0.0103
Length O_7···N_9 (Å)	2.826	2.823
Angle between O_7-H_8···N_9 (°)	143.519	143.957
[b]Downshifted stretch frequency O_7-H_8 (cm^{-1})	215	250

[a]O_7-H_8 bond length of aa – ee rotamer. [b]O_7-H_8 frequency of ee – aa rotamer.

The results confirmed that the expected *J* values are not affected by the solvent or that the dielectric continuum model fails to promote the geometrical changes. Thus, the aa were the lowest in energy in non-polar and polar solvents. This shortcoming can be attributed, in this case, to the approach in neglecting the explicit solute-solvent interactions contributions. Therefore, the implicit solvation model correctly describes the aa conformer as more stable in non-polar solvents due to IAHB but, it wrong represents the aa as more stable in polar solvents, where solute-solvent interactions should dominate, leading to more stability of ee conformer.

Therefore, to probe the conformational changes in solution, we used the expected *J* values calculated in gas phase along with the experimental data. This was accomplished through the measurement of coupling constant in solvent of different polarity ($^3J_{obs}$) and the molar fractions (X) for ee and aa conformers were determined through Equation (3):[53,54]

Table 5. Calculated coupling constants[a] for most stable conformers of the compounds *cis*-3-EACOL and *cis*-3-DEACOL solvated by SMD model

Compound	Solvent/gas phase	$^3J_{H1a/H2a}$	$^3J_{H1e/H2e}$
cis-3-EACOL	CCl_4	10.10	3.00
	DMSO-d_6	10.46	4.00
	Gas phase	11.16	4.13
cis-3-DEACOL	CCl_4	9.60	3.50
	DMSO-d_6	9.80	3.50
	Gas phase	11.13	4.14

[a]In Hz.

$$X_{ee} = (^3J_{obs} - {}^3J_{H1e/H2e})/(^3J_{H1a/H2a} - {}^3J_{H1e/H2e}) \quad (3)$$

The $J_{H1e/H2e}$ and $J_{H1a/H2a}$ are the calculated coupling constants in gas phase for the ee and aa conformers individually obtained from the weighted average over all rotamers using Equation (4), where p_{Ri} represented the thermal population (see supplementary material) and ^3J_i the intrinsic coupling constant of rotamer *i* in the conformational equilibrium.

$$^3J_{H1a/H2a \text{ and } H1e/H2e} = \sum_{i=1}^{n} p_{Ri}\ {}^3J_i \quad (4)$$

Since $X_{ee} + X_{aa} = 1$, the free energy difference ($\Delta G°$) can be readily obtained from Equation (5), where R = 0.00199 kcal mol^{-1} K^{-1}, T = 298 K and $K_1 = X_{ee}/X_{aa}$.

$$\Delta G° = -RT\ln K \quad (5)$$

The results presented in Table 6 show that *cis*-3-EACOL has a very high proportion of the aa conformation in non-polar solvents (92% in CCl_4; $\Delta G_{ee\text{-}aa}$ = 1.48 kcal mol^{-1}). In polar solvents, the ee conformation predominates (90% in DMSO-d_6; $\Delta G_{ee\text{-}aa}$ = −1.31 kcal mol^{-1}). These results show that in non-polar solvents, the equilibrium of *cis*-3-EACOL is more displaced for the aa conformation, and there is less solvation of the substituent groups. This favors the formation of the IAHB OH···N, which becomes more important than the

Table 6. Experimental hydrogen H1 and H3 coupling constants[a], molar fractions (X_{ee}), and the equilibrium free energies ($\Delta G_{ee\text{-}aa}$)[b] for *cis*-3-EACOL in solvents[c] of different dielectric constants (ε) and basicities (SB)[d]

Solvent	SB	ε	$^3J_{H1/H2a}$	$^3J_{H1/H2e}$	$^3J_{H3/H2a}$	$^3J_{H3/H2e}$	X_{ee}	ΔG
CCl_4	0.04	2.24	4.67	4.67	4.54	4.54	0.08	1.48
$CDCl_3$	0.07	4.81	6.16	3.24	6.15	3.20	0.29	0.54
$C_2D_2Cl_4$	---	8.50	7.09	3.48	7.13	3.52	0.42	0.19
CD_3CN	0.29	37.50	8.67	3.41	---	---	0.65	−0.36
Acetone-d_6	0.48	20.70	9.04	3.49	---	---	0.69	−0.50
Pyridine-d_5	0.58	12.40	9.81	3.79	9.94	3.65	0.81	−0.85
DMSO-d_6	0.65	46.70	10.46	4.00	10.70	3.70	0.90	−1.31

[a]In Hz; calculated coupling constants in gas phase using Equation (2): $^3J_{H1a/H2a}$ = 11.16 Hz; $^3J_{H1e/H2e}$ = 4.13 Hz. [b]In kcal mol^{-1}. [c]Concentration: 0.05 mol L^{-1}. [d]Ref. 55.

Table 7. Experimental hydrogen H1 and H3 coupling constants[a], molar fractions (X_{ee}), and the equilibrium free energies ($\Delta G_{ee\text{-}aa}$)[b] for *cis*-3-DEACOL in solvents[c] of different dielectric constants (ε) and basicities (SB)[d]

Solvent	SB	ε	$^3J_{H1/H2a}$	$^3J_{H1/H2e}$	$^3J_{H3/H2a}$	$^3J_{H3/H2e}$	X_{ee}[b]	ΔG[b,c]
CCl_4	0.04	2.24	8.70	4.26	---	---	0.64	−0.33
$CDCl_3$	0.07	4.81	8.50	4.18	---	---	0.61	−0.26
CD_3CN	0.29	37.50	10.41	4.12	11.08	3.43	0.89	−1.25
Acetone-d_6	0.48	20.70	10.52	4.15	11.31	3.34	0.91	−1.36
Pyridine-d_5	0.58	12.40	10.67	4.18	11.55	3.33	0.93	−1.55

[a]In Hz; calculated coupling constants in gas phase using Equation (2): $^3J_{H1a/H2a}$ = 11.13 Hz; $^3J_{H1e/H2e}$ = 4.14 Hz. [b]In kcal mol^{-1}. [c]Concentration: 0.05 mol L^{-1}. [d]Ref. 55.

syn-1,3-diaxial steric effect between the substituent groups and the axial hydrogens.

For *cis*-3-DEACOL (Table 7) the proportion of ee is 64% in CCl_4 ($\Delta G_{ee\text{-}aa}$ = −0.33 kcal mol^{-1}) and increases to 93% in pyridine-d_5 ($\Delta G_{ee\text{-}aa}$ = −1.55 kcal mol^{-1}). These results indicate that although the IAHB OH···N is present, the *syn*-1,3-diaxial steric effect is predominant in this equilibrium.

Comparing $^3J_{HH}$ values for hydrogen H-1 in CCl_4 of *cis*-3-EACOL ($^3J_{H1/H2a}$ or $^3J_{H1/H6a}$ = 4.67 Hz) and *cis*-3-DEACOL ($^3J_{H1/H2a}$ or $^3J_{H1/H6a}$ = 8.70 Hz), along with the literature results for *cis*-3-aminocyclohexanol (7.46 Hz),[49] *cis*-3-*N*,*N*-dimethyl-aminocyclohexanol (7.50 Hz),[28] it was observed that for secondary amino groups, the strength of the IAHB OH···N is predominant over the steric effect. For the tertiary amino groups, which are bulkier than the secondary amino groups, the 1,3-diaxial steric effect is predominant.

Analysis of the solvent effect also showed that the $^3J_{HH}$ values increase as the solvent basicity increases (SB),[55] not with the increasing dielectric constant (ε). For example, the diequatorial conformer proportion for *cis*-3-EACOL in pyridine (ε = 12.40, SB = 0.58) is 81%, while in CDCN (ε = 37.50, SB = 0.29) this value is 65%.

CONCLUSIONS

The theoretical calculations showed that the IAHB influences the conformational equilibria of these compounds, stabilizing the aa conformer. The change from -NHC_2H_5 to the -$N(C_2H_5)_2$ substituent increased the strength of the IAHB due to hyperconjugative interactions and inductive effects. However, the proportion of the aa conformation decreased from 96% to 41% of *cis*-3-EACOL to *cis*-3-DEACOL compound, because the 1,3-diaxial steric effect is also strengthened. Although the implicit solvation model fails to predict the conformational changes, combining experimental NMR data in solution and computed *J*-couplings in gas phase, qualitative trends of conformational preference of the compounds could be described. The results indicated that the aa conformer is favored in less polar solvents (92% and 36% for *cis*-3-EACOL and *cis*-3-DEACOL in CCl_4). However, with an increase in solvent polarity, the ee conformation showed a high population in the equilibria (81% and 93% for *cis*-3-EACOL and *cis*-3-DEACOL in pyridine-d_5).

SUPPLEMENTARY MATERIAL

Electronic supplementary material associated with this article can be found at http://quimicanova.sbq.org.br, in pdf format, with free access.

ACKNOWLEDGMENTS

The authors thank CAPES for fellowships (P. R. B and G. J. C.). P. R. B also thanks the São Paulo Research Foundation (FAPESP) grant #2021/09687-5 for financial support. We also gratefully acknowledge CENAPAD-SP for the use of computer facilities.

REFERENCES

1. Sachse, H.; *Ber. Dtsch. Chem. Ges.* **1890**, *23*, 1363. [Crossref]
2. Solha, D. C.; Barbosa, T. M.; Viesser, R. V.; Rittner, R.; Tormena, C. F.; *J. Phys. Chem. A* **2014**, *118*, 2794. [Crossref]
3. Anizelli, P. R.; Vilcachagua, J. D.; Cunha Neto, A.; Tormena, C. F.; *J. Phys. Chem. A* **2008**, *112*, 8785. [Crossref]
4. Barbosa, T. M.; Viesser, R. V.; Abraham, R. J.; Rittner, R.; Tormena, C. F.; *RSC Adv.* **2015**, *5*, 35412. [Crossref]
5. Tormena, C. F.; *Prog. Nucl. Magn. Reson. Spectrosc.* **2016**, *96*, 73. [Crossref]
6. Melo, U. Z.; Fernandes, C. S.; Francisco, C. B.; Carini, T. C.; Gauze, G. F.; Rittner, R.; Basso, E. A.; *J. Phys. Chem. A* **2020**, *124*, 8509. [Crossref]
7. Fabiola, F.; Bertram, R.; Korostelev, A.; Chapman, M. S.; *Protein Sci.* **2002**, *11*, 1415. [Crossref]
8. Bordo, D.; Argos, P.; *J. Mol. Biol.* **1994**, *243*, 504. [Crossref]
9. Fersht, A. R.; Serrano, L.; *Curr. Opin. Struct. Biol.* **1993**, *3*, 75. [Crossref]
10. Batista, P. R.; Karas, L. J.; Viesser, R. V.; de Oliveira, C. C.; Gonçalves, M. B.; Tormena, C. F.; Rittner, R.; Ducati, L. C.; Oliveira, P. R.; *J. Phys. Chem. A* **2019**, *123*, 8583. [Crossref]

11. Cacela, C.; Duarte, M. L.; Fausto, R.; *Spectrochim. Acta, Part A* **2000**, *56*, 1051. [Crossref]
12. Thomsen, D. L.; Axson, J. L.; Schrøder, S. D.; Lane, J. R.; Vaida, V.; Kjaergaard, H. G.; *J. Phys. Chem. A* **2013**, *117*, 10260. [Crossref]
13. Khalil, A. S.; Kelterer, A. M.; Lavrich, R. J.; *J. Phys. Chem. A* **2017**, *121*, 6646. [Crossref]
14. Cormanich, R. A.; Ducati, L. C.; Rittner, R.; *Chem. Phys.* **2011**, *387*, 85. [Crossref]
15. Cormanich, R. A.; Ducati, L. C.; Rittner, R.; *J. Mol. Struct.* **2012**, *1014*, 12. [Crossref]
16. Cormanich, R. A.; Ducati, L. C.; Tormena, C. F.; Rittner, R.; *Chem. Phys.* **2013**, *421*, 32. [Crossref]
17. Kakeshpour, T.; Bailey, J. P.; Jenner, M. R.; Howell, D. E.; Staples, R. J.; Holmes, D.; Wu, J. I.; Jackson, J. E.; *Angew. Chem.* **2017**, *56*, 9842. [Crossref]
18. Wu, J. I.; Jackson, J. E.; Schleyer, P. V. R.; *J. Am. Chem. Soc.* **2014**, *136*, 13526. [Crossref]
19. Kakeshpour, T.; Wu, J. I.; Jackson, J. E.; *J. Am. Chem. Soc.* **2016**, *138*, 3427. [Crossref]
20. Ganguly, A.; Paul, B. K.; Guchhait, N.; *Comput. Theor. Chem.* **2017**, *1117*, 108. [Crossref]
21. Karas, L. J.; Batista, P. R.; Viesser, R. V.; Tormena, C. F.; Rittner, R.; de Oliveira, P. R.; *Phys. Chem. Chem. Phys.* **2017**, *19*, 16904. [Crossref]
22. Ebrahimi, S.; Dabbagh, H. A.; Eskandari, K.; Hernández-Trujillo, J.; Christiansen, O.; Francisco, E.; Pendás, A. M.; Rocha-Rinza, T.; Kim, K.; Inoue, Y.; *Phys. Chem. Chem. Phys.* **2016**, *18*, 18278. [Crossref]
23. Kolahdouzan, K.; Ogba, O. M.; O'Leary, D. J.; *J. Org. Chem.* **2022**, *87*, 1732. [Crossref]
24. Oliveira, P. R.; Rittner, R.; *J. Mol. Struct.* **2005**, *743*, 69. [Crossref]
25. Oliveira, P. R.; Rittner, R.; *Spectrochim. Acta, Part A* **2005**, *61*, 1737. [Crossref]
26. Oliveira, P. R.; Ortiz, D. S.; Rittner, R.; *J. Mol. Struct.* **2006**, *788*, 16. [Crossref]
27. Oliveira, P. R.; Rittner, R.; *Spectrochim. Acta, Part A* **2008**, *70*, 1079. [Crossref]
28. Oliveira, P. R.; Ribeiro, D. S.; Rittner, R.; *J. Phys. Org. Chem.* **2005**, *18*, 513. [Crossref]
29. Rackers, J. A.; Laury, M. L.; Lu, C.; Wang, Z.; Lagardère, L.; Piquemal, J. P.; Ren, P.; Ponder, J. W.; *TINKER 8*; The University of Texas at Austin and Sorbonne Universités, 2018.
30. Zhao, Y.; Truhlar, D.; *Theor. Chem. Acc.* **2008**, *120*, 215. [Crossref]
31. Walker, M.; Harvey, A. J. A.; Sen, A.; Dessent, C. E. H.; *J. Phys. Chem. A* **2013**, *117*, 12590. [Crossref]
32. Jensen, F.; *Introduction to Computacional Chemistry*, 2nd ed.; Wiley: Chichester, 2007.
33. Becke, A. D.; *J. Chem. Phys.* **1993**, *98*, 5648. [Crossref]
34. Lee, C.; Yang, W.; Parr, R. G.; *Phys. Rev. B* **1988**, *37*, 785. [Crossref]
35. Vosko, S. H.; Wilk, L.; Nusair, M.; *Can. J. Phys.* **1980**, *58*, 1200. [Crossref]
36. Stephens, P. J.; Devlin, F. J.; Chabalowski, C. F.; Frisch, M. J.; *J. Phys. Chem.* **1994**, *98*, 11623. [Crossref]
37. Barone, V.; *J. Chem. Phys.* **1994**, *101*, 6834. [Crossref]
38. Barone, V. In *Recent Advances in Density Functional Methods, Part I*, Chong, D. P., ed.; World Scientific: Singapore, 1996.
39. Suardíaz, R.; Pérez, C.; Crespo-Otero, R.; Vega, J. M. G.; Fabián, J. S.; *J. Chem. Theory Comput.* **2008**, *4*, 448. [Crossref]
40. Marenich, A. V.; Cramer, C. J.; Truhlar, D. G.; *J. Phys. Chem. B*. **2009**, *113*, 6378. [Crossref]
41. Frisch, M. J.; Trucks, G. W.; Schlegel, H. B.; Scuseria, G. E.; Robb, M. A.; Cheeseman, J. R.; Scalmani, G.; Barone, V.; Mennucci, B.; Petersson, G. A.; Nakatsuji, H.; Caricato, M.; Li, X.; Hratchian, H. P.; Izmaylov, A. F.; Bloino, J.; Zheng, G.; Sonnenberg, J. L.; Hada, M.; Ehara, M.; Toyota, K.; Fukuda, R.; Hasegawa, J.; Ishida, M.; Nakajima, T.; Honda, Y.; Kitao, O.; Nakai, H.; Vreven, T.; Montgomery Junior, J. A.; Peralta, J. E.; Ogliaro, F.; Bearpark, M. J.; Heyd, J.; Brothers, E. N.; Kudin, K. N.; Staroverov, V. N.; Kobayashi, R.; Normand, J.; Raghavachari, K.; Rendell, A. P.; Burant, J. C.; Iyengar, S. S.; Tomasi, J.; Cossi, M.; Rega, N.; Millam, N. J.; Klene, M.; Knox, J. E.; Cross, J. B.; Bakken, V.; Adamo, C.; Jaramillo, J.; Gomperts, R.; Stratmann, R. E.; Yazyev, O.; Austin, A. J.; Cammi, R.; Pomelli, C.; Ochterski, J. W.; Martin, R. L.; Morokuma, K.; Zakrzewski, V. G.; Voth, G. A.; Salvador, P.; Dannenberg, J. J.; Dapprich, S.; Daniels, A. D.; Farkas, Ö.; Foresman, J. B.; Ortiz, J. V.; Cioslowski J.; Fox, D. J.; *Gaussian09, Revision D.01*; Gaussian, Inc., Wallingford, 2009.
42. Glendening, E. D.; Badenhoop, J. K.; Reed, A. E.; Carpenter, J. E.; Bohmann, J. A.; Morales, C. M.; Landis, C. R.; Weinhold, F.; *NBO 6.0*; Theoretical Chemistry Institute, Madison, 2013.
43. Bader, R. F. W.; *Chem. Rev.* **1991**, *91*, 893. [Crossref]
44. Keith, T. A.; *AIMALL, version 11.10.16*; TK Gristmill Software, Overland Park, 2011.
45. Contreras-García, J.; Johnson, E. R.; Keinan, S.; Chaudret, R.; Piquemal, J. P.; Beratan, D. N.; Yang, W.; *J. Chem. Theory Comp.* **2011**, *7*, 625. [Crossref]
46. Eusebio, J.; Muñiz, O. M.; *Rev. Soc. Quim. Mex.* **2001**, *45*, 218. [Link] accessed in April 2023
47. Koch, U.; Popelier, P. L. A.; *J. Phys. Chem.* **1995**, *99*, 9747. [Crossref]
48. Badenhoop, J. K.; Weinhold, F.; *J. Chem. Phys.* **1997**, *107*, 5406. [Crossref]
49. Cremer, D.; Kraka, E.; *Angew. Chem.* **1984**, *23*, 627. [Crossref]
50. Espinosa, E.; Alkorta, I.; Rozas, I.; Elguero, J.; Molins, E.; *Chem. Phys. Lett.* **2001**, *336*, 457. [Crossref]
51. Paul, B. K.; Guchhait, N.; *Chem. Phys.* **2012**, *403*, 94. [Crossref]
52. Ruud, K.; Frediani, L.; Cammi, R.; Mennucci, B.; *Int. J. Mol. Sci.* **2003**, *4*, 119. [Crossref]
53. Oliveira, P. R.; Viesser, R. V.; Guerrero Junior, P. G.; Rittner, R.; *Spectrochim. Acta, Part A* **2011**, *78*, 1599. [Crossref]
54. Haasnoot, C. A. G.; de Leeuw, F. A. A. M.; Altona, C.; *Tetrahedron* **1980**, *36*, 2783. [Crossref]
55. George, W.; *Handbook of Solvents*, Reprinted ed.; ChemTec Publishing: Toronto, 2001.